On the Convergence of the Physico-Chemical Properties of [*n*]Helicenes

Lubomír Rulíšek,* Otto Exner, Lukasz Cwiklik, Pavel Jungwirth, Ivo Starý, and Zdeněk Havlas

Institute of Organic Chemistry and Biochemistry Academy of Sciences of the Czech Republic, Gilead Sciences Research Center & IOCB, and Center for Complex Molecular Systems and Biomolecules, Flemingovo nam. 2, 166 10 Praha 6, Czech Republic

Abstract: The results of a series of DFT and DFT-D calculations are reported with the aim to predict the physico-chemical properties (equilibrium structures, stabilization energies, redox potentials, excitation and CD spectra, electronic conductivity, and elasticity) of elongating helical structures (i.e., [*n*]helicenes, *n*= 1-14). It was shown that many of them are converged at [14]helicene: the interpitch distance to the value of R_{pitch} = 3.75 Å; the incremental stabilization energy ΔG_n to the value of 11 kJ.mol^{-1} (thus suggesting the inherent destabilization of the growing helical structures); the S_0-S_1 energy difference to the estimated band gap of 2.60 eV; and redox potentials corresponding to the reduction of [*n*]helicenes to E^0 = -2.2 V. The elasticity was shown to decrease as a linear function *m* (i.e., $k \approx m$) with k = 0.01056 a.u. for [14]helicene. Moreover, the conductivity properties were discussed in terms of hole and excess electron densities. Possible implications of the calculated data in nanoscience are discussed.

* Corresponding author. Tel. (Fax): +420–220 183 263 (299). E-mail: lubos@uochb.cas.cz

1. Introduction

The chiral molecules of helicenes[1] attract attention as simple models for screw-shaped biomolecules, such as proteins and nucleic acids. Recently, they have been recognized as potential building blocks in nanomaterial sciences[2] and the interest in their chemistry and physico-chemical properties has remarkably increased.[3] The pioneering synthesis and resolution of hexahelicene by Newman and Lednicer more than fifty years ago[4] was afterward followed by successful photochemistry-based attempts at the preparation of a nearly homologous series of [*n*]helicenes up to *n* = 14 (ref. 5). However, the Martin's photochemical approach to helicenes,[6] which has been substantially improved by Katz,[7] suffers from several serious drawbacks as it is not general and, even more seriously, high dilution conditions to suppress polymerisation of the starting material make it extremely laborious. Naturally, the alternative approaches to helicenes have recently emerged and at least two of them have been found to be more general as Diels-Alder reaction of aromatic vinylethers with *p*-benzoquinone developed by Katz[8] and intramolecular [2+2+2] cyclisation of aromatic triynes in the presence of Ni^0 or Co^I complexes.[9] From the practical point of view, helicenes as unique 3-D polyaromatic systems are chemically stable, soluble in common organic solvents, and π-conjugated materials. This sets them apart from planar polyaromatic systems, which are often insoluble and unstable as, *i.e.*, higher acenes. Thus, helicenes represent an attractive objective for further research in various branches of chemistry and nanoscience, as the area of their application is evidently underdeveloped.

Experimental efforts were complemented by many theoretical studies: Furche *et al.*[10] have carried out time-dependent density functional theory (TD-DFT) calculations in order to investigate electronic circular dichroism (CD) spectra of helicenes; similar efforts were taken by Autsbach *et al.*[11] Electronic properties of helicenes, such as electronic conductance of the growing helical system, was subject of the study of Treboux *et al.*[12] and the local stability of [*n*]acenes, [*n*]phenacenes, and [*n*]helicenes (*n* =1-9) was addressed by Portella et al.[13]

The original systematic quantum chemical investigation of the stability of [*n*]helicenes was published by Schulman and Disch.[14] They calculated energies of [6]helicene to [10]helicene at the B3LYP/6-311G(d,p) level, together with their magnetic properties and ^{1}H NMR shifts, and compared the results with the isomeric [*n*]phenacenes. However, it must be noted that although the DFT calculations are well suited particularly for the relative values of the energies (substituent effects),[15,16,17] their accuracy can be insufficient for calculations of stabilization of molecules containing strong non-bonding intramolecular interactions. Thus, in our previous study,[18] we addressed the computational and methodological aspects of quantum chemical calculations of helical systems. It was shown that the accurate electronic structure calculation of the extended helical structure is a non-trivial issue. This is mainly due to problems with the correct description of the interpitch stabilization and the considerable intramolecular basis set superposition error[19] experienced by post-SCF methods, such as MP2 and CCSD(T) methods, which leads to an artificial overstabilization of the helical systems. In contrast, DFT calculations tend to significantly underestimate the intramolecular stabilization, which makes any predictions regarding the incremental stabilization of [*n*]helicenes questionable. Both problems are resolved using the DFT-D method, which includes the empirical dispersion energy terms into the DFT calculation,[20] and yields accurate structures and energies.

The second reason why these calculations shall be revisited is the fact that only the total molecular energy was analyzed in the series of [*n*]helicenes and [*n*]phenacenes with increasing *n*, and therefore, any finer effect of structure was masked by the trivial dependence on the molecular weight.[21,22] On the contrary we calculated here the differences between two following members of the helicene series, using the framework of isodesmic[23,24] (and homodesmic[24]) reactions, in which a polycyclic hydrocarbon is synthesized from the lower aromatic homologue. This principle was used in previous studies of various substituent effects in organic molecules.[16,17,22]

We further extended the series of investigated compounds to lower members up to phenanthrene and added calculations of redox potentials, singlet-triplet energy gaps, elasticity, and

electronic conductivity in connection with possible application for nanomaterials. We expect to obtain a comprehensive picture about the convergence of the physico-chemical properties of [*n*]helicenes.

2. Computational details

All density functional theory (DFT) and MP2 calculations reported in the study were carried out using the program Turbomole 5.7.[25] The Perdew-Burke-Ernzerhof (PBE)[26] and B3LYP functionals[27] have been used throughout. The DFT/PBE and MP2 calculations were expedited by expanding the Coulomb integrals in an auxiliary basis set, the resolution-of-identity (RI-J) approximation[28,29] The method is denoted as RI-PBE or RI-MP2. All the geometry optimizations were carried out using the 6-31G(d) basis set,[30] whereas the single point energies were recomputed using a larger TZVP (triple-zeta valence with one polarization function on each atom) basis set.[31] Furthermore, to account for dispersion forces, representing an important stabilizing factor in the studied systems (which are not described by the currently used DFT functionals), empirical dispersion parameters were added both to energy and gradients during geometry optimization and during the calculations of the single point energies.[32,33]

In the atomic dispersion scheme the total dispersion energy is calculated as a sum of all possible pair-wise atomic contributions:

$$E_{\text{dis}} = -\sum_{i<j} f_{\text{damp}}(r_{ij}, R_{ij}^{0}) \frac{C_{ij}}{r_{ij}^{6}} \qquad (1)$$

The value of E_{dis} is simply added to the total DFT energy, and the gradient of the dispersion energy is added to the quantum mechanical gradient during the optimization. In Eq. 1,

$$f_{\text{damp}} = \frac{1}{1 + e^{-d\left(\frac{r_{ij}}{s_R R_{ij}^{0}} - 1\right)}} \qquad (2)$$

is a damping function similar to that introduced by Grimme.[32] This method is denoted as DFT-D and the full set of parameters, including the combination rules for R^0_{ij} and C_{ij} can be found in ref. 33.

To account for the effects of the environment, the conductor-like screening model (COSMO)[34,35] was used with the dielectric constant corresponding to acetonitrile ($\varepsilon_r = 36.6$) as a typical polar organic solvent. The Gibbs free energy was then calculated as the sum of the following contributions:

$$G = E_{el(+D)} + G_{solv} + (E_{ZPE} + nRT - TS), \qquad (3)$$

where $E_{el(+D)}$ is the *in vacuo* energy of the system (including empirical dispersion energy corrections in case of DFT-D method), calculated at the B3LYP/TZVP level at the geometry optimized at the RI-PBE/6-31G(d) level), G_{solv} is the solvation free energy (calculated at the RI-PBE/6-31G(d) level) and the (E_{ZPE} + nRT – TS) term contains the zero-point energy, thermal corrections to the Gibbs free energy and the entropic term (obtained from a frequency calculation with the same method and software as for the geometry optimizations at the RI-PBE/6-31G(d) level, 298.15 K and 1 atm pressure, using the harmonic oscillator-rigid rotor-ideal gas approximation.[36]

The redox potentials were then calculated according to the equation:

$$E^0\,[\mathrm{V}] = 27.21(G_{ox}\,[\mathrm{a.u.}] - G_{red}\,[\mathrm{a.u.}]) - 4.43\ \mathrm{V}, \qquad (4),$$

where $G_{ox/red}$ are free energy values of the oxidized and reduced forms calculated according to Eq. (1), and 4.34 V is an absolute redox potential of the standard hydrogen electrode (SHE).[37]

In order to interpret and predict the spectra of studied molecules, the TD-DFT method[38,39,40,41] as implemented in the Turbomole program[10] was used in conjunction with the B3LYP functional.

The homodesmic reaction used for the definition of ΔE_n, i. e., the measure of the stabilization energy of [n]helicenes and [n]phenacenes is depicted in Scheme 1.

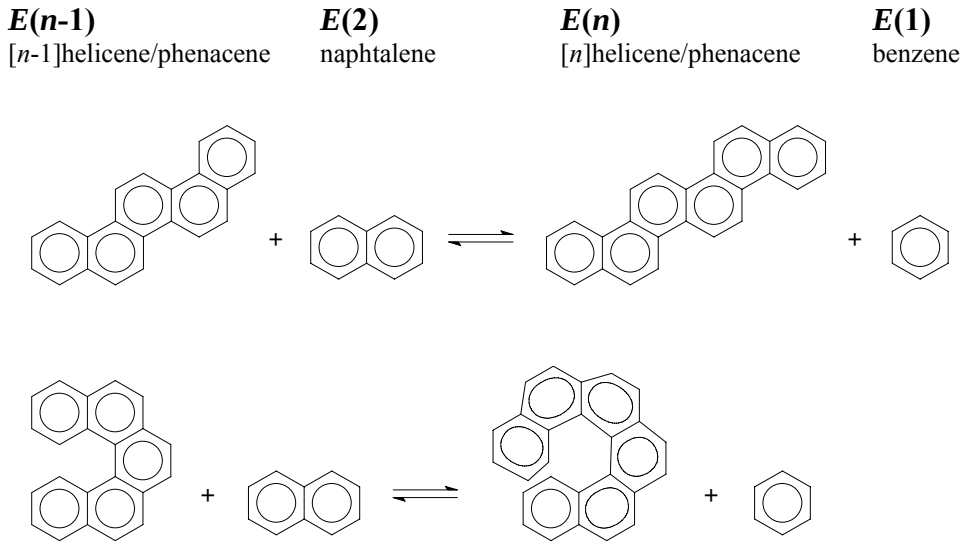

5

6

$$\Delta E_n = E(n) + E(1) - E(n\text{-}1) - E(2)$$

Scheme 1. The homodesmic addition of naphthalene to [*n*-1]helicene (phenacene) yielding [*n*]helicene (phenacene) and benzene molecules, used for the definition of stability of growing helical structure (ΔE_n).

3. Results and Discussion

3.1. Molecular geometry.

A key parameter describing the helical structure is the interpitch distance. The definition of this distance, used for the purposes of this work, is given in Figure 1 together with the definition of the twist angle ϕ that describes the deviation from the ideal helix containing 6 benzene rings per turn (thread). Its definition is meaningful starting from [7]helicene. As has been shown in our previous work,[18] only the DFT-D method predicts this distance in a good agreement with the

experimental values (c.f., R_{pitch}(exp) = 4.50 Å *vs.* R_{pitch}(MP2) = 3.91 Å, R_{pitch}(DFT) = 4.93 Å, R_{pitch}(DFT-D) = 4.64 Å for [7]helicene structure).

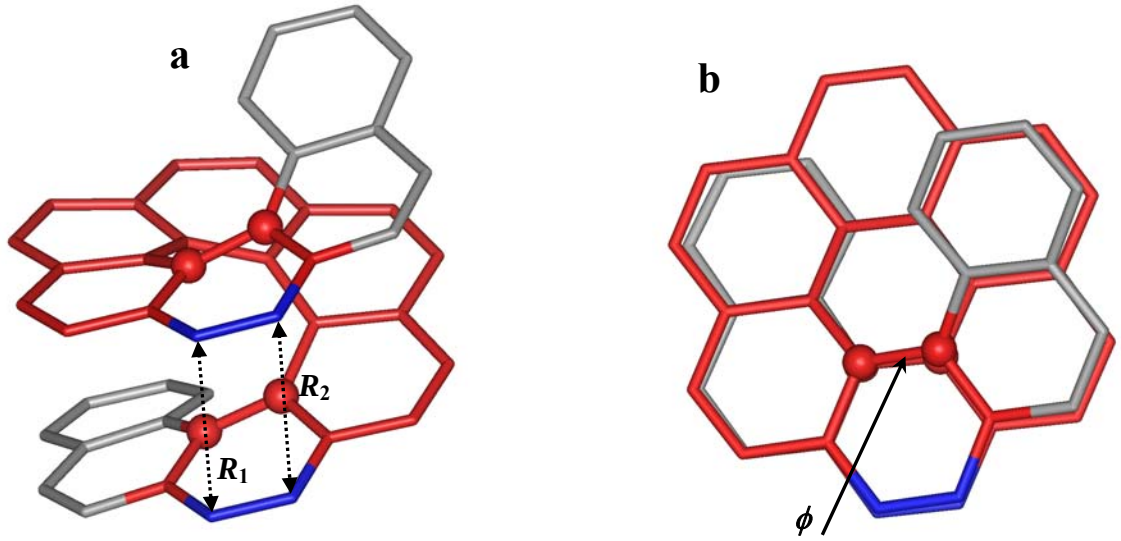

Figure 1: The definition of the interpitch distance (R_{pitch}) and twist angle (ϕ) demonstrated on the example of [11]helicene (top and side view, hydrogens not displayed). (a) R_{pitch} = (R_1 + R_2)/2, where R_1 and R_2 describe [n…(n+7)] distance in the core region of the helicene, which is defined as the region with equal number of benzene rings on both ends (for [2i+1]helicenes) or (k,k+1) rings (for [2i]helicenes). (b) the twist angle ϕ is the dihedral angle between four carbon atoms highlighted with balls.

The values of the interpitch distances (R_{pitch}) and the average twist angles over the core region (ϕ) are given in Table 1 for neutral helicenes, their anions, and cations.

Table 1: The calculated values of R_{pitch} (in Å) and twist angle ϕ) for neutral helicenes, their anions and cations, as defined in Fig. 1. The positive value of the twist angle indicates that there are more than six benzene units per one helical turn.

	[*n*]helicene$^{(-)}$		[*n*]helicene		[*n*]helicene$^{(+)}$	
n	R_{pitch}(Å)	ϕ(deg)	R_{pitch}(Å)	ϕ(deg)	R_{pitch}(Å)	ϕ(deg)
7	4.64	-0.7	4.64	1.9	4.41	4.9
8	4.10	-2.6	4.21	2.2	4.25	8.2
9	3.78	-1.6	3.90	2.5	3.97	6.9
10	3.68	-3.0	3.82	3.1	3.76	0.9
11	3.61	-3.0	3.74	3.5	3.81	8.5
12	3.63	-1.8	3.75	4.3	3.69	2.4
13	3.67	-1.2	3.76	5.1	3.75	3.0
14	3.66	-0.8	3.75	5.4	3.65	3.0

It can be seen that the values of R_{pitch} converge to the value of ~3.75 Å for neutral helicenes, and to ~3.65 Å for their anions and cations. Interestingly, for neutral [*n*]helicenes and the cations, the values of twist angles are positive, indicating there are slightly more that six benzene rings in one helical turn (thread) (~6.05-6.08), whereas in the anionic structures the turn is completed with marginally less than six benzene rings (~5.98 units/turn). However, the twist angles do not converge as smoothly as the R_{pitch} distances. The simple extrapolation of the calculated values predicts that at ~ [80]helicene, a shift of one benzene ring can occur. Due to the poor convergence of the twist angles, this prediction is, however, not highly reliable.

3.2. Inherent stability of helical structures.

The relative stabilization energy ΔE_n of an [*n*]helicene (or [*n*]phenacene), related to the [*n*–*1*] homologue is expressed as the reaction energy of the isodesmic reaction, in which the helicenes is produced from its lower homologue (*viz* Scheme1). The calculated values of ΔE_n and the Gibbs free energies ΔG_n are listed in Table 2; ΔE_n are plotted in Figure 2 (with respect to *n*).

Table 2: The comparison of the calculated ΔE_n and ΔG_n values for the hypothetical (isodesmic) addition of naphthalene to [*n*-1]helicene yielding [*n*]helicene and benzene molecules (reaction **2** in Scheme 1). All values are in kJ.mol^{-1}.

	[*n*]helicenes				[*n*]phenacenes			
	DFT(PBE)+D		DFT(B3LYP)+D		DFT(PBE)+D		DFT(B3LYP)+D	
n	ΔE_n	ΔG_n	ΔE_n	ΔG_n	ΔE_n	ΔG_n	ΔE_n	ΔG_n
3[a]	-5.6	-5.5	-6.1	-6.0	-5.6	-5.5	-6.1	-6.0
4	21.0	24.5	23.3	26.8	-0.5	-1.3	0.2	-0.6
5	15.3	17.1	17.3	19.1	-2.1	-2.0	-1.8	-1.7
6	7.8	9.8	9.1	11.0	-1.9	-2.5	-1.3	-2.0
7	7.1	8.7	9.8	11.4	-1.8	-1.6	-1.6	-1.4
8	4.6	8.1	6.9	10.4	-1.9	-2.3	-1.4	-1.8
9	3.6	7.8	5.4	9.6	-1.7	-1.7	-1.4	-1.4
10	5.9	9.5	8.0	11.6	-1.9	-2.4	-1.5	-2.0
11	5.8	8.4	8.0	10.6	-1.8	-1.9	-1.5	-1.6
12	5.3	9.1	7.1	11.0	-1.8	-2.2	-1.5	-1.8
13	5.7	9.0	7.3	10.5	-1.8	-1.7	-1.4	-1.4
14	5.7	10.9	7.5	12.7	-1.9	-2.3	-1.5	-1.9

[a] [3]helicene = [3]phanecene = phenanthrene

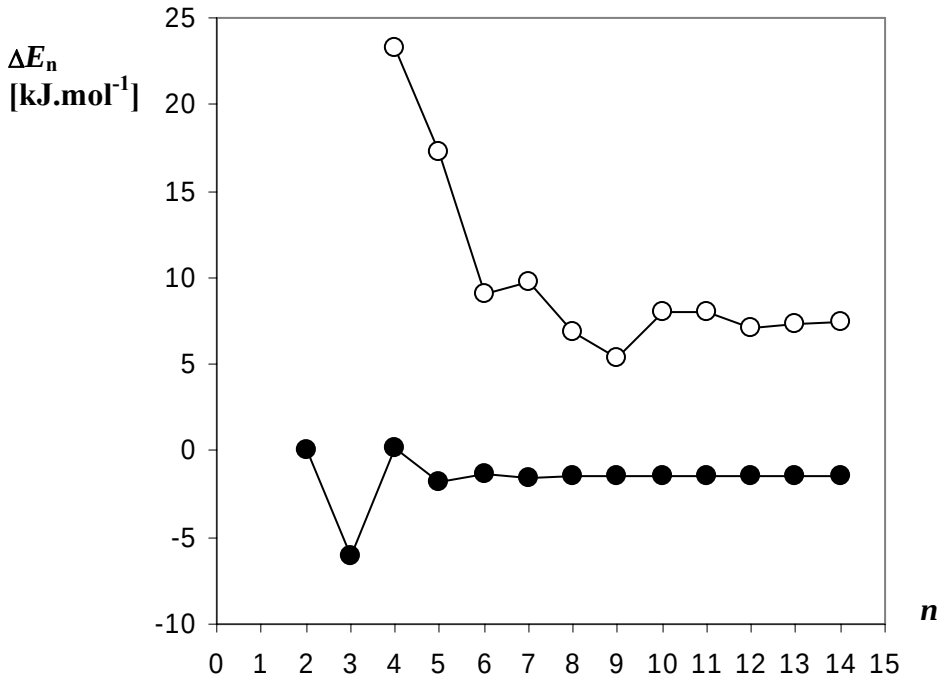

Figure 2: Relative energies ΔE_n of [*n*]phenacenes ● and [*n*]helicenes ○, as defined in Scheme 1, plotted with respect to the number of benzene rings *n*.

As can be seen in Fig. 2, the molecules of phenacenes are slightly stabilized with each added benzene ring by a practically constant amount of energy. This is in agreement with the

classical theory of Clar[42] that predicts the larger stability the more virtual benzene rings can be written in the molecular structure. The significant stabilization of phenanthrene is also in accord with Clar's theory. On the contrary, the molecules of helicenes are destabilized by a variable energy increase ΔE_n (4 to 23 kJ mol^{-1}); with greater *n* they tend to converge to a constant value. The steric tension is well expressed in the steadily increasing total energy. One can thus understand that higher members of this series are difficult to synthesize but the synthesis should not be prevented when starting from the previous homologue. The Clar theory does not account for nonplanar molecules; there is also no simple explanation why [9]helicene and [8]helicene are somewhat more stable than the other members of the series. The difference between isomeric helicene and phenacene is according to our calculations increasing by ~10 kJ mol^{-1} per unit, which is significantly smaller than the value of Schulman and Disch[14] (26 kJ mol^{-1}) obtained with somewhat insufficient theoretical model.

The most remarkable feature that can be seen in Fig. 2 is the larger value of ΔE_n for [4]helicene (benzo[c]phenanthrene). Although the steric hindrance is only due to interaction of two hydrogen atoms, the energy increase is rather large; when the molecule becomes nonplanar, addition of further benzene rings has much smaller effect. A nonplanar structure of this compound was revealed by X-ray diffraction[43] and the experimental twisting angle agrees with our calculations.

Our approach offered an opportunity to calculate the "aromatic character" based on the theoretically calculated (but observable) quantities. Among the various definitions, the index HOMA (harmonic oscillator model aromaticity) of Krygowski[44,45] (Eq. 7 below) defined purely on the molecular geometry, meets this condition. In Eq. 7, $\alpha = 257.7$ is an empirical constant and the C–C bond lengths R_i are given in Å. The value of 1.388 Å corresponds to the C-C bond length in benzene. One can calculate the aromatic character of the whole molecule or of a particular ring; the summation extends accordingly.

$$\mathrm{HOMA} = (\alpha/n)\Sigma(1.388 - R_i)^2 \qquad (7)$$

The values of HOMA index calculated either for the whole molecule or for the end ring are depicted in Figure 3. Most conspicuous is the behavior of phenanthrene, whose aromatic character is low but that of the terminal rings is high. This is again in agreement with the Clar theory, which describes the structure of phenanthrene as near to two benzene rings connected with a double bond. The increase of aromatic character in [4]phenacene is also in agreement with this theory (increased number of structures with entire benzene rings); it is observed even in [4]helicene in spite of the steric hindrance. In general the difference between helicenes and phenacenes is small; as a matter of fact it is much smaller than differences between the individual rings, terminal and internal, in the same molecule. It was observed for several physical quantities that the nonplanar structure of helicenes has only moderate effect on the inhibition of resonance.

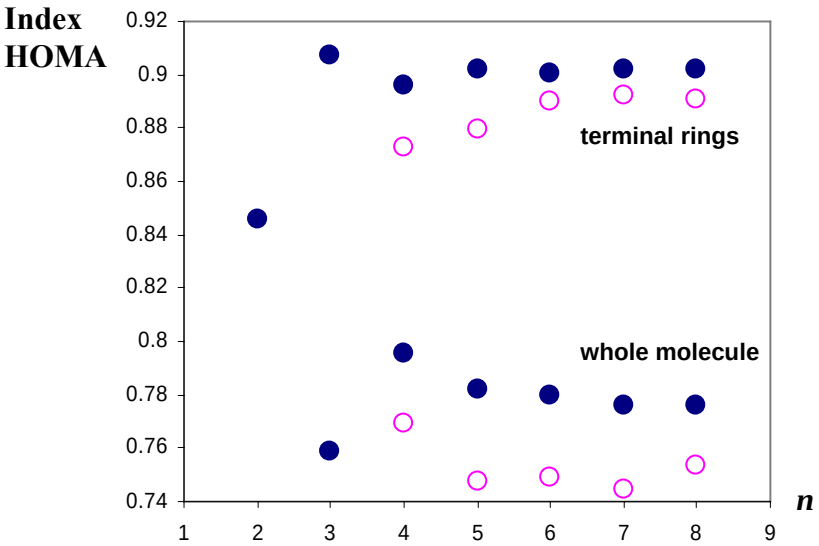

Figure 3: The index of aromaticity (HOMA) of [*n*]phenacenes ● and [*n*]helicenes ○, plotted vs the number of benzene rings n; at the bottom for the whole molecule, at the top for the terminal rings.

3.3. Optical and CD electronic spectra: TD-DFT and CASPT2 calculations.

The optical and CD electronic spectra for [*n*]helicenes (*n* = 4-7, 12) have been reported by Furche *et al.*[10] It has been shown that TD-DFT method yields the results in a good agreement with experimental data. Here, the calculations are extended to cover the whole series of studied [*n*]helicenes (*n* = 4-14) and include the lowest triplet states of all the systems. The results are compiled in Table 3 for the six lowest singlets and the lowest triplet state.

Table 3: The excitation energies (in nm) of (P)-[*n*]helicenes calculated by TD-DFT method using B3LYP functional. The six lowest singlet states and the first triplet are reported. For each singlet excitation, the oscillator strengths *f* (in dipole-length representation), and rotatory strengths (*R* is in 10^{-40} cgs units) are listed as well.

\[*n*] State	[4]	[5]	[6]	[7]	[8]	[9]	[10]	[11]	[12]	[13]	[14]
S_1	350	377	394	416	430	441	451	458	464	471	476
F	6.10^{-4}	0.001	0.003	2.10^{-4}	0.001	1.10^{-5}	7.10^{-4}	8.10^{-5}	5.10^{-5}	4.10^{-6}	8.10^{-4}
R	0.13	-3	0.6	-0.9	4.3	-0.07	14	-0.8	-0.4	0.11	5.6
S_2	340	353	375	393	409	425	434	449	454	467	471
F	0.02	0.009	0.001	0.01	0.002	0.03	5.10^{-4}	0.017	2.10^{-5}	0.007	5.10^{-7}
R	-19	-0.95	-2.1	109	-8.6	444	-3.9	242	-0.15	109	-0.11
S_3	288	329	346	387	404	419	432	439	449	453	461
F	0.8	0.32	0.32	0.08	0.08	0.016	0.05	0.03	0.04	0.03	0.03
R	112	347	638	492	780	275	760	507	708	548	549
S_4	285	318	337	362	384	404	413	426	435	445	454
F	0.1	0.06	0.05	0.05	0.015	0.014	0.003	0.003	2.10^{-4}	1.10^{-4}	5.10^{-4}
R	-73	-98	-87	64	-58	51	-27	-43	-12	6.7	11
S_5	272	312	328	357	378	396	410	423	429	433	441
F	0.005	0.025	0.004	0.01	0.004	0.02	0.003	0.001	0.001	2.10^{-4}	9.10^{-5}
R	-6	10	39	-27	33	-89	41	-4	10	1.4	-1.6
S_6	271	304	322	350	364	384	397	409	424	433	435
F	0.006	4.10^{-4}	0.04	0.04	0.016	0.01	0.016	0.001	4.10^{-4}	1.10^{-5}	3.10^{-6}
R	11	-1.6	-48	-61	-30	-54	-112	-24	-8	1	-0.13
T_1	447	429	465	470	487	495	502	508	514	516	522

The calculated TD-DFT/B3LYP/TZVP results are in a very good agreement with experimental data available for tetra- (372, 328, 295, 282, 274 nm),[46] penta- (396, 344, 310 nm),[47] hexa- (412, 347, 325, -, 314 nm),[48] and heptahelicenes (422, -, 386, 364 nm).[49,50] This gives us confidence in predicting the trends for higher helicenes (n > 7). Not surprisingly, the values of excitation energies monotonically shift to the longer wavelengths. In all cases, the most intense peak is predicted for the S_3 state ($2B_1$ state in the C_2 symmetry point group), which shifts from 288 nm to 461 nm ([14]helicene). Its intensity is decreasing, whereas the rotatory strengths R are approximately conserved over the studied helicene series. The range of excitation energies for S_1-S_6 states is narrowed (from 80 to 40 nm). For the [14]helicene, the computed excitation energy correspond to the band gap of 2.60 eV, which is rather close to the predicted value of 2.49 eV for [∞]helicene.[12] The singlet-triplet energy gaps are also monotonically decreasing over the studied series, however it is not predicted that $S_0 \rightarrow T_1$ excitation energy can be half of the $S_0 \rightarrow S_1$ to indicate that helicenes can be potential candidates for singlet fission mechanism which can be used for better efficiency of fotovoltaic cells.[51]

3.4. Redox Potentials: experimental and theoretical data.

The convergence of the redox potentials, ionization potentials and electron affinities over the studied series of helical structures was investigated. The calculated data are compiled in Table 4. The redox potentials (in acetonitrile solution) were calculated both for the hypothetical oxidation and reduction of helicenes. It can be seen that the values of redox potentials corresponding to the reduction of helicenes, i.e., to the process

$$[n]\text{helicene} + e^- \rightarrow [n]\text{helicene}^-$$

converge to the values of $E^0 \approx -2.2$ V, the redox potentials corresponding to the oxidation process

$$[n]\text{helicene} - e^- \rightarrow [n]\text{helicene}^+$$

are still decreasing (E^0 = 0.65 V for [14]helicene). Since the same holds true for electron affinities (converging to ~0.85 eV) and ionization potentials (IP([14]helicene) = 6.26 eV), the observed trends can be clearly attributed to the electronic structure effects (and not solvation of the systems). It can be concluded that over the studied series, it is easier to oxidize the helical structures, whereas their reduction can be more difficult to achieve.

Table 4: The redox potentials, ionization potentials and electron affinities of [*n*]helicenes calculated by DFT/B3LYP method. The reported values of E^0 are in mV and related to standard hydrogen electrode (SHE).

[*n*]	E^0 (reduction)	E^0 (oxidation)	**EA** (in eV)	$\mathbf{IP_{adiabatic}}$ (eV)
[4]	-2.305	1.199	0.23	7.16
[5]	-2.288	1.141	0.33	6.99
[6]	-2.174	1.080	0.53	6.88
[7]	-2.142	0.994	0.63	6.75
[8]	-2.115	0.963	0.66	6.68
[9]	-2.118	0.891	0.75	6.57
[10]	-2.098	0.809	0.75	6.51
[11]	-2.131	0.803	0.82	6.43
[12]	-2.128	0.749	0.80	6.39
[13]	-2.146	0.909	0.86	6.34
[14]	-2.159	0.646	0.85	6.26

3.5. Electronic structure of parent and dearomatized helicenes

We asked ourselves how does the conductivity of helicenes[12] qualitatively reflect itself in the electronic structure and how can it be affected by sequential dearomatization of one to three benzene rings. To this end, we investigated the [7]helicene and a series of its four derivatives with an increasing number of dearomatized rings (see Table 5 for the number and position(s) of the dearomatized rings). The geometry of each structure described in Table 5 was optimized at the RI-DFT-D/PBE/6-31G(d) level. After optimization, single point energy calculations at the RI-MP2/6-

31G(d) level were performed not only for the neutral molecule, but also for the corresponding cation and anion (in the geometry of neutral system). This allowed us to evaluate the hole density as the difference of the electron density of the cation minus that of the neutral molecule and the excess electron density as the difference of the electron density of the anion minus that of the neutral molecule. Note that these are measurable quantities, which in our view provide a much better picture of electron delocalization and conductivity properties than one would get from the (strictly speaking) non-measurable frontier orbitals, HOMO and LUMO.

Table 5: Notation of the studied systems with the number and position(s) of the dearomatized rings.

Symbol	number of dearomatized rings	position(s) of dearomatized rings
[7]helicene	0	-
[7]helicene-D1	1	4
[7]helicene-D2	2	2, 6
[7]helicene-D3a	3	2, 4, 6
[7]helicene-D3b	3	3, 4, 5

The hole and excess electron densities for the molecules presented in Table 5 are shown in Figure 4. For all systems, the hole and excess electron densities correlate well with each other in terms of localization vs. delocalization, providing a simple representation of the conductivity properties of these molecules. In the parent helicene (Figure 4a) the hole and the excess electron are, as expected, completely delocalized over the whole system, which underlines the conductive character of helicens. Dearomatizing the central benzene ring (Figure 4b) leads to structuring of the hole or excess electron density with significant depletion (particularly for the latter case) at the dearomatized ring. The structuring process is further exemplified when two separate rings are dearomatized (Figure 4c), however, it takes at least three dearomatized rings to fully break the hole

and, particularly, excess electron densities into disconnected pieces (Figures 4d-4e). Particularly, when the three central adjacent rings are dearomatized (Figure 4e) the densities effectively break into two parts and the molecule starts resembling a classical donor-acceptor pair separated by a spacer group. Clearly, conductivity will be lost in this system.

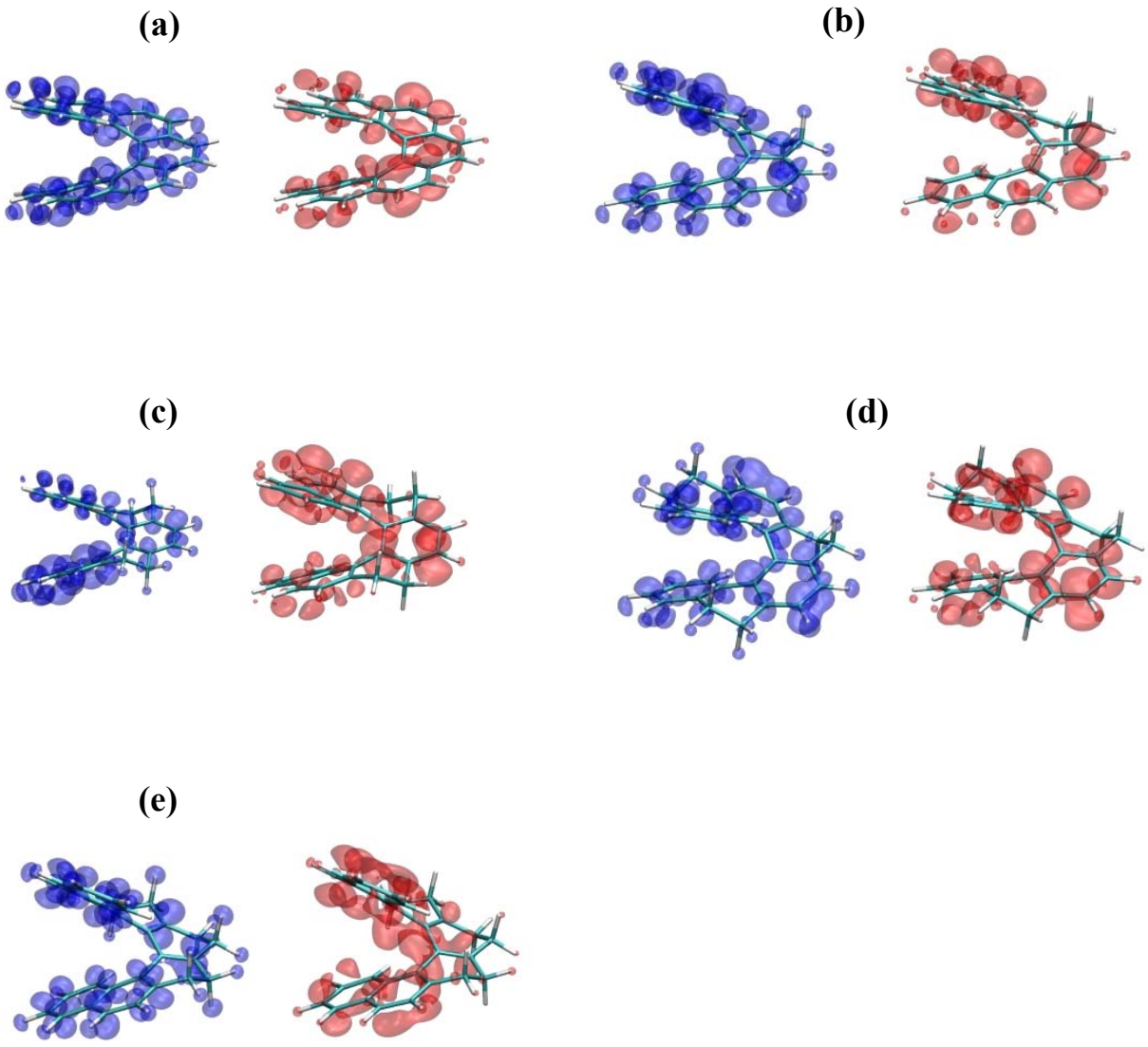

Figure 4: Hole (blue) and excess electron (red) densities (0.002 isovalue) for (a) [7]helicene, (b) [7]helicene-D1, (c) [7]helicene-D2, (d) [7]helicene-D3a, and (e) [7]helicene-D3b.

3.6. Low-lying vibrational states. An assessment of elasticity of helical structures.

In order to predict the behavior of helical structures with respect to their potential use as molecular strings, a normal mode analysis has been carried out for all the studied helicenes. Not surprisingly, it turned out that the lowest vibrational modes correspond to the deformation of the helical skeleton. Mostly, these are linear combinations of symmetric and antisymmetric stretching modes along the *z*-axis and twisting of the helical screw (i.e., the motions in the *xy* plane). Starting from [9]helicene, we were able, in all cases, to identify a low-lying vibrational mode that can be described as the symmetric stretching of the helical skeleton. This mode has been found at an almost constant frequency of ~55 cm^{-1} with respect to *n* in the series of [*n*]helicenes (*n* = 9 – 14). This suggests a decreasing elasticity of the growing helical structure (i.e., increasing force constant *k*, since $\omega_0 = \sqrt{(k/m)}$), if the helicene is viewed as a molecular string.[52]

In order to separate the motion in the *z*-dimension, we have carried out a computational experiment with [14]helicene by stretching the structure along the *z*-axis. The distance *R*, defined and depicted in Figure 5b has been changed from its equilibrium value of 6.88 Å down to 5.98 Å and up to 7.78 Å (13 points in total). The resulting potential energy curve along this coordinate is depicted in Figure 5a. It enables us to predict the harmonic force constant (according to the Hooke's law) k = 0.01056 a.u. (99 $kJ.mol^{-1}.Å^{-2}$) for the helical stretching, corresponding to a frequency of 67 cm^{-1}, which is reasonably close to 55 cm^{-1} estimated above. In order to compare this calculated value to that for other helical structures, we used the Hooke's law $E = (1/2L_0)Y_f(L-L_0)^2$ from the mechanics of continuum which defines the force constant Y_f as the 'property of the material', independent of the length L_0. This yields the value of Y_f = 11 300 pN, which is approximately ten times higher than that for the 'average' DNA helix.[53]

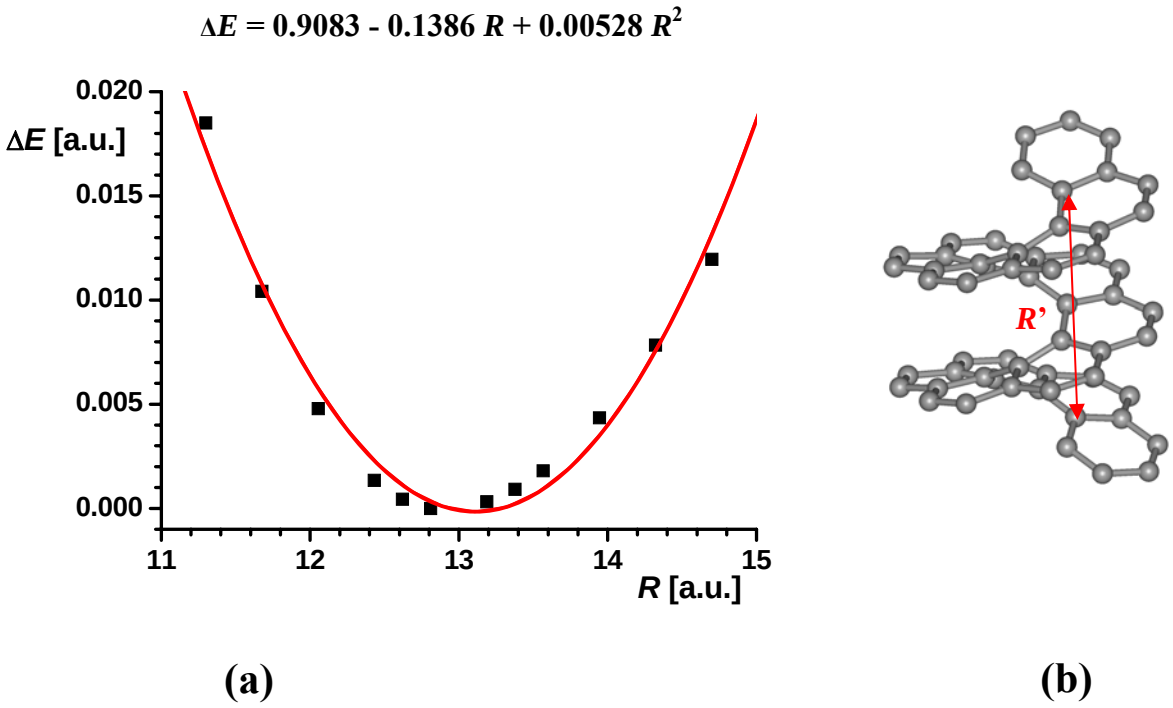

Figure 5: The calculated energy change corresponding to the stretching of [14]helicene along the *z*-axis. The distance *R*' is defined in the right part of the figure.

4. Conclusions

Since helicenes can be considered as the potential building blocks of nanomaterial structures,[2] we have systematically investigated the convergence of their physico-chemical properties with the number of aromatic rings. It was shown that many of their properties are already reasonably converged at the [14]helicene. The equilibrium structures tend undergo a contraction along the *z*-axis with the R_{pitch} (interpitch distance) converging to the value of 3.75 Å for [14]helicene. However, the value of incremental stabilization energy (ΔG_n, defined as the free energy change upon addition of the naphtalene to [*n*]helicene to obtain [*n*+1]helicene and benzene) converge to the value of +11 kJ.mol^{-1}, which suggests that the synthesis of long helical structures can be more difficult to accomplish. Calculations of electronic and CD spectra converge fairly rapidly with system size to the value of the estimated band gap (2.60 eV). The redox potential

corresponding to oxidation of the helicenes continues to decrease (with E^0 = 0.65 V for [14]helicene), whereas the redox potentials for the helicene reduction converge to the values of ~ -2.2 V. The conductivity properties of helicenes were qualitatively discussed in terms of hole and excess electron densities. It was also demonstrated how the conductive character is disappearing upon dearomatization of one to three benzene rings of the helicene molecule. The elasticity of the growing helical structure is decreasing with n and ω_0 (corresponding to the symmetric stretching along z-axis) is equal to ~55 cm^{-1}. The two force constants were calculated as k = 0.01056 a.u. (99 $kJ.mol^{-1}.Å^{-2}$) and Y_f = 11 300 pN for [14]helicene, which implies that the elasticity of higher helicenes is about ten times lower than that of DNA helices.

Acknowledgment. This work was supported by projects LC512 and Z4 055 0506, and the program KONTAKT ME 857 of Czech Ministry of Education.

Supporting Information Available. The equilibrium geometries of all the studied molecules are available free of charge via the Internet at http://pubs.acs.org.

References

(1) (a) Laarhoven, W. H.; Prinsen, W. J. C. *Top. Curr. Chem.* **1984**, 125, 63. (b) Meurer, K. P.; Vögtle, F. *Top. Curr. Chem.* **1985**, *127*, 1. (c) Oremek, G.; Seiffert, U.; Janecka, A. *Chem.-Ztg*. **1987**, *111*, 69. (d) Vögtle, F. *Fascinating Molecules in Organic Chemistry*; Wiley: New York, 1992; p 156. (e) Hopf, H. *Classics in Hydrocarbon Chemistry: Syntheses, Concepts, Perspectives*; VCH: Weinheim, 2000; Chapter 12.2, p 323.

(2) Verbiest, T.; Van Elshocht, S.; Kauranen, M.; Hellemans, L.; Snauwaert, J.; Nuckolls, C.; Katz, T. J.; Persoons, A. *Science* **1998**, *282*, 913. (b) Treboux, G.; Lapstun, P.; Wu, Z. H.; Silverbrook, K. *Chem. Phys. Lett*. **1999**, *301*, 493. (c) Kelly, T. R.; Silva, R. A.; De Silva, H.; Jasmin, S.; Zhao, Y. *J. Am. Chem. Soc*. **2000**, *122*, 6935. (d) Botek, E.; Champagne, B.; Turki, M.; Andre, J. M. *J. Chem. Phys*. **2004**, *120*, 2042.

(3) (a) Katz, T. J. *Angew. Chem., Int. Ed.* **2000**, *39*, 1921. (b) Urbano, A. *Angew. Chem. Int. Ed.* **2003**, *42*, 3986.

(4) Newman, M. S.; Lednicer, D. *J. Am. Chem. Soc.* **1956**, *78*, 4765.

(5) Martin, R. H.; Baes, M. *Tetrahedron* **1975**, *31*, 2135.

(6) Flammang-Barbieux, M.; Nasielski, J.; Martin, R. H. *Tetrahedron Lett.* **1967**, 743.

(7) Liu, L.; Yang, B.; Katz, T. J.; Poindexter, M. K. *J. Org. Chem.* **1991**, *56*, 3769.

(8) Willmore, N. D.; Liu, L. B.; Katz, T. J. *Angew. Chem., Int. Ed*. **1992**, *31*, 1093.

(9) (a) Stará, I. G.; Alexandrová, Z.; Teplý, F. ; Sehnal, P. ; Starý, I.; Šaman, D.; Buděšínský, M.; Cvačka, J. *Organic Lett*. **2005**, *13*, 2547. (b) Teplý, F.; Stará, I. G.; Starý, I.; Kollárovič, A.; Šaman, D.; Fiedler, P.; Vyskočil, Š. *J. Org. Chem*. **2003**, *68*, 5193. (c) Teplý F.; Stará, I. G.; Starý, I.; Kollárovič, A.; Šaman, D.; Rulíšek, L.; Fiedler, P. *J. Am. Chem. Soc*. **2002**, *124*, 9175.

(10) Furche, F.; Ahlrichs, R.; Wachsmann, C.; Weber, E.; Sobanski, A.; Vögtle, F.; Grimme, S. *J. Am. Chem. Soc.* **2000**, *122*, 1717-1724.

(11) Autschbach, J.; Ziegler, T.; van Gisbergen, S. J. A.; Baerends, E. J. J. Chem. Phys. 2002, 116, 6930-6940.

(12) Treboux, G.; Lapstun, P.; Wu, Z.; Silverbrook, K. *Chem. Phys. Lett.* **1999**, *301*, 493-497.

(13) Portella, G.; Poater, J.; Bofill, J. M.; Alemany, P.; Solà, M. *J. Org. Chem.* **2005**, *70*, 2509-2521.

(14) Schulman, J. M.; Disch, R. L. *J. Phys. Chem. A* **1999**, *103*, 6669-6672.

(15) Wiberg, K. B. *J. Org. Chem.* **2002**, *67*, 4787.

(16) Exner, O.; Böhm, S. *Phys. Chem. Chem. Phys.* **2004**, *6*, 3864.

(17) Böhm, S.; Exner, O. *J. Comput. Chem.* **2006**, *27*, 571.

(18) Rulíšek, L.; Valdés, H.; Klusák, V.; Exner, O.; Starý, I.; Hobza, P. *J. Comput. Chem.* **2007***, submitted*.

(19) Jensen, F. *Chem. Phys. Lett.* **1996**, *261*, 633-636.

(20) Grimme, S. *J. Comput. Chem.* **2006**, *27*, 1787-1799.

(21) Exner, O. Collect. *Czech Chem. Commun.* **1966**, *31*, 3222.

(22) Exner, O. *J. Phys. Org. Chem.* **1997**, *10*, 797.

(23) Pross, A.; Radom, L.; Taft, R. W. *J. Org. Chem.* **1980**, *45*, 818.

(24) George, P.; Trachtman, M.; Bock, C. W.; Brett, A. M. *J. Chem. Soc.-Perkin Trans. 2* **1976**, 1222.

(25) Ahlrichs, R.; Bär, M.; Häser, M.; Horn, H.; Kölmel, C. *Chem. Phys. Lett.* **1989** *162*, 165.

(26) Perdew, J. P.; Burke, K.; Ernzerhof, M. *Phys. Rev. Lett.*, **1996**, *77*, 3865-3868.

(27) (a) A. D. Becke, *Phys. Rev. A* **1988**, *38*, 3098-3100. (b) C. T. Lee, W. T. Yang, R. G. Parr, *Phys. Rev. B* **1988**, *37*, 785-789. (c) A. D. Becke, *J. Chem. Phys.* **1993**, *98*, 5648-5652.

(28) Eichkorn, K.; Treutler, O.; Öhm, H.; Häser, M.; Ahlrichs, R. *Chem. Phys. Lett.* **1995**, *240*, 283-290.

(29) Eichkorn, K.; Weigen, F.; Treutler, O.; Ahlrichs, R. *Theor. Chim. Acta* **1997**, *97*, 119-124.

(30) Hehre, W. J.; Radom, L.; Schleyer, PI. v. R.; Pople, J. A. *Ab initio molecular orbital theory*; Wiley-Interscience: New York, 1986.

(31) Schäfer, A.; Huber, C.; Ahlrichs, R. *J. Chem. Phys.* **1994**, *100*, 5829.

(32) Grimme, S. *J. Comput. Chem.* **2004**, *25*, 1463.

(33) Jurečka, P.; Černý, J.; Hobza, P.; Salahub, D. *J. Comput. Chem.* **2007**, *28*, 555-569.

(34) Klamt, A.; Schuurmann, G. *J. Chem. Soc.-Perkin Trans. 2* **1993**, 799-805.

(35) Schäfer, A.; Klamt, A.; Sattel, D.; Lohrenz, J. C. W.; Eckert, F. *Phys. Chem. Chem. Phys.* **2000,** *2*, 2187-2193.

(36) Jensen, F. *Introduction to Computational Chemistry*; John Wiley & Sons, 1999.

(37) Reiss, H.; Heller, A. *J. Phys. Chem.* **1985**, *89*, 4207-4213.

(38) Runge, E.; Gross, E. K. U. *Phys. Rev. Lett.* **1984**, *52*, 997.

(39) Gross, E. K. U.; Kohn, W. *Adv. Quantum Chem.* **1990**, *21*, 255.

(40) Casida, M. E. Time-Dependent Density Functional Response Theory for Molecules. In *Recent advances in density functional methods*; Chong, D. P., Ed.; World Scientific: Singapore, 1995; Vol. 1.

(41) Gross, E. K. U.; Dobson, J. F.; Petersilka, M. *Top. Curr. Chem.* **1996**, *181*, 81.

(42) Clar, E. *Aromatic Hydrocarbons*, Academic Press, London, 1964.

(43) Lakshman, M. K.; Kole, P. L.; Chaturvedi, S.; Saugier, J. H.; Yeh, H. J. C.; Glusker, J. P.; Carrell, H. L.; Katz, A. K.; Afshar, C. E.; Dashwood, W.-M.; Kenniston, G.; Baird, W. M. *J. Am. Chem. Soc*. **2000**, *122*, 12629.

(44) Krygowski, T. M. *J. Chem. Inf. Comp. Sci.* **1993**, *33*, 70.

(45) Krygowski, T. M.; Cyrański, M. *Tetrahedron* **1996**, *52*, 1713.

(46) Jones, R. N.; Spinner, E. *Spectrochim. Acta* **1960**, *16*, 1060.

(47) Brown, A.; Kemp, C. M.; Mason, S. F. *J. Chem. Soc. A* **1971**, 751.

(48) Weigang, O. E., Jr.; Trouard Dodson, P. A. *J. Chem. Phys.* **1968**, *49*, 4248.

(49) Brickell, W. S.; Brown, A.; Kemp, C. M.; Mason, S. F. *J. Chem. Soc. A* **1971**, 756.

(50) Palewska, K.; Chojnacki, H. *Mol. Cryst. Liq. Cryst.* **1993**, *229*, 31.

(51) (a) Gratzel, M. *Nature* **2001**, *414*, 338. (b) Paci, I.; Johnson, J. C.; Chen, X.; Rana, G.; Popovic, D.; David, D. E.; Nozik, A. J.; Ratner, M. A.; Michl, J. *J. Am. Chem. Soc*. **2006**, *128*, 16546-16553.

(52) Jalaie, M.; Weatherhead, S.; Lipkowitz, K. D.; Robertson, D. *Electronic J. Theor. Chem.* **1997**, *2*, 268-272.

(53) Kubař, T.; Hanus, M.; Ryjáček, F.; Hobza, P. *Chem. Eur. J.* **2006**, *12*, 280-290.